

**Electronic Restructuring in Shape-Memory Alloys:  
Thermodynamic and electronic structure studies of the  
martensitic transition**

J. C. Lashley, R. K. Schulze, B. Mihaila, W. L. Hulst, J. C. Cooley, and J. L. Smith  
*Los Alamos National Laboratory, Los Alamos, NM 87545, USA*

P. S. Riseborough  
*Physics Department, Temple University, Philadelphia, PA 19122, USA*

C. P. Opeil  
*Department of Physics, Boston College, Chestnut Hill, MA 02467, USA*

R. A. Fisher  
*Lawrence Berkeley National Laboratory, Berkeley, California 94720, USA*

O. Svitelskiy and A. Suslov  
*National High Magnetic Field Laboratory,  
Florida State University, Tallahassee, FL 32310, USA*

T. R. Finlayson  
*School of Physics, Monash University, Clayton, Victoria, Australia 3800*

(Dated: November 12, 2018)

## Abstract

Using a variety of thermodynamic measurements made in magnetic fields, we show evidence that the diffusionless transition (DT) in many shape-memory alloys is related to significant changes in the electronic structure. We investigate three alloys that show the shape-memory effect (In-24 at.% Tl, AuZn, and U-26 at.% Nb). We observe that the DT is significantly altered in these alloys by the application of a magnetic field. Specifically, the DT in InTl-24 at.% shows a decrease in the DT temperature with increasing magnetic field. Further investigations of AuZn were performed using an ultrasonic pulse-echo technique in magnetic fields up to 45 T. Quantum oscillations in the speed of the longitudinal sound waves propagating in the [110] direction indicated a strong acoustic de Haas-van Alphen-type effect and give information about part of the Fermi surface.

PACS numbers: 71.20.Be, 75.40.-s, 75.47.Np

## I. INTRODUCTION

Martensitic transitions (MTs) are diffusionless structural transitions that generally occur between a high-temperature cubic phase and a lower-temperature phase with a lower symmetry. The MT proceeds via an atomic rearrangement that involves a collective shear displacement and shows almost no change in volume. Often the MT can be preceded by a higher temperature pre-MT. According to Friedel<sup>1</sup>, the martensitic transition is entropy driven. In Friedel's picture, the high-temperature cubic structure is stabilized by the entropy of low-frequency phonon modes, and the low-temperature close-packed structure is energetically stable due to the larger coordination number. Measurements of the elastic constants<sup>2,3</sup> and the phonon-dispersion relations<sup>3,4,5</sup> show the existence of anomalies in the high-temperature phases. In these bcc phases, the transverse acoustic phonon frequencies are observed to soften<sup>6,7</sup> as the temperature is reduced towards the MT temperature, but generally the softening is incomplete since it is arrested by the MT before the phonon frequency reaches zero<sup>8,9</sup>. Presumably the incomplete softening is a result of anharmonic interactions, which would also be in accord with the transition being of first-order and not continuous. The observed partial softening can be used to infer the symmetry of the low-temperature structure<sup>10,11,12</sup>. The entropy deduced from the phonon density of states for most shape-memory alloys has been found to account for 65% to 75% of the total entropy change at the transition, and can be as high as 90% in Cu-based shape-memory alloys<sup>13</sup>.

The above picture has led to theoretical models<sup>14,15</sup> that describe the transition entirely in terms of entropy and anharmonic lattice dynamics. However the entropy-driven scenario is deficient because the explanation does not explicitly address the energetic stability of the close-packed phases at low-temperature. It has been found that it is the difference in the electronic energies that dominate the structural stability energy of transition metals<sup>16</sup>. The above statement is also true for simple metals<sup>17,18</sup> since the lattice or Madelung energies of the body centered and the close-packed structures are extremely close<sup>19,20</sup>. In fact, it has long been known that in Hume-Rothery alloys, the electron concentration per atom is extremely important in determining which structure is stable<sup>21</sup>. Shortly after Hume-Rothery's discovery, Jones suggested that the stability<sup>22</sup> of the crystal structure could be understood in terms of an energy lowering due to the Fermi surface being close to the active Brillouin zone boundaries. Although Jones's simple one-electron picture has been shown

to be deficient<sup>23</sup>, it still provides a remarkably good phenomenological description of these materials. Because many MTs proceed by shuffles (that is displacements involving quasi-static phonons with (fractional) commensurate wave vectors with uniform shears<sup>24</sup>), it is possible that the electron concentration could also play an important role in producing the phonon anomalies of martensitic Hume-Rothery alloys. Recently, there have been an increasing number of investigations that emphasize the importance of the electronic structure. Transport measurements have shown that significant changes occur in the magnetoresistance of AuZn alloys, which imply that significant changes in the Fermi surface have taken place<sup>25</sup>. De Haas-van Alphen measurements<sup>26</sup> made above and below the MT temperature showed drastic reconstruction of the Fermi surface, thereby confirming the conclusions of McDonald *et al.*<sup>25</sup>. Electronic-structure calculations<sup>27</sup> indicate that Fermi-surface nesting may also be responsible for the phonon softening observed<sup>28</sup> in the pre-martensitic phases of NiTi, NiAl, and AuCd alloys, as well as that predicted for vanadium and niobium at high pressure<sup>29</sup>. The electronic momentum distribution has been measured for a NiAl alloy by Compton-scattering experiments<sup>30</sup>, which allowed the Fermi surface to be mapped out and which shows indications of nesting in agreement with the theoretical predictions of Zhao and Harmon<sup>27</sup>.

In this paper, we report thermodynamic measurements in magnetic fields on three non-magnetic alloys that show the shape-memory effect. These measurements demonstrate that magnetic-field-induced changes of the electronic structure strongly couple to the DT. Acoustic de Haas-van Alphen measurements, which are a direct probe of the Fermi surface, on AuZn using pulse-echo sound-speed measurements in high-magnetic fields provide further evidence of the important role of the conduction electrons in the DT. We show in AuZn that the velocities of the longitudinal acoustic phonons depend on the magnetic field and that the phonon frequencies exhibit an oscillatory dependence on the inverse of the magnetic field. This phenomenon is understood<sup>31</sup> as a consequence of successive Landau tubes sweeping through the Fermi surface, which modulate the dielectric constant at the reciprocal lattice vectors and, through the screening of the pair potential, modulate the observed phonon velocities. This interpretation is in accord with the observation<sup>32</sup> that (in InTl alloys) Kohn anomalies in the phonon-dispersion relations occur at wave vectors almost commensurate with reciprocal lattice vectors.

## II. THERMAL-EXPANSIVITY MEASUREMENTS

The coefficient of linear thermal expansion,  $\alpha$ , was measured in a three-terminal capacitive dilatometer<sup>33</sup> over the range  $100\text{ K} \leq T \leq 300\text{ K}$ . The specimen was held against a rigid fixed platform on the bottom, and the top was in contact with a spring-loaded lower capacitor plate, which was located below an upper capacitor plate. As the specimen expanded and contracted, it changed the size of the gap  $D$  between the capacitor plates. It should be noted that there is an unavoidable constant stress to the sample from the spring connecting to the lower capacitor plate. This stress is the same from measurement to measurement. Because the temperature dependence of this capacitance includes contributions from the specimen and the cell, the cell effect is measured separately and subtracted. Capacitance was measured with a Andeen-Hagerling 2500 A 1 kHz ultra-precision capacitance bridge. Data were recorded on cooling at a rate of 0.2 K/min, and the bridge was set to take 10 averages at each point.

The performance of the cell was tested against an aluminum standard, and the measurements fell within 1% of the reference material. With this apparatus, the operative equation to obtain the thermal expansion is

$$\alpha = \frac{1}{L} \frac{d}{dT} [D_c - D_s] + \alpha_{Cu}. \quad (1)$$

Here,  $L$ , denotes specimen length at room temperature,  $D_c$ , the gap from the cell effect,  $D_s$ , the gap from the expansion or contraction of the specimen, and,  $\alpha_{Cu}$ , the coefficient of linear thermal expansion for copper. The sample was a single crystal of an InTl alloy with 24 at. % Tl which is a composition in the range where the high-temperature fcc phase becomes unstable to an fct phase at lower temperatures<sup>34</sup>. Following the standard explanation of the tetragonal distortion<sup>35</sup>, one expects that the fct phase is stabilized by large gaps in the electronic dispersion relations at the Bragg planes derived from the  $\{111\}$  and  $\{200\}$  reciprocal lattice vectors of the fcc structure. Since the  $c/a$  ratio is greater than unity in the tetragonally distorted phase<sup>36</sup>, it may also be expected that the (200) and (020) reciprocal lattice vectors should move closer to  $2k_F$  in the tetragonal phase, while (002) moves in the opposite direction. The results of the thermal-expansivity measurements on an InTl alloy with 24 at. % Tl are shown in Fig. 1. The sample was oriented with a  $[100]$  axis of the fcc structure parallel to the axis of the capacitor. Thermal- expansivity measurements were performed with decreasing temperature, once with zero field and once with a field of  $H =$

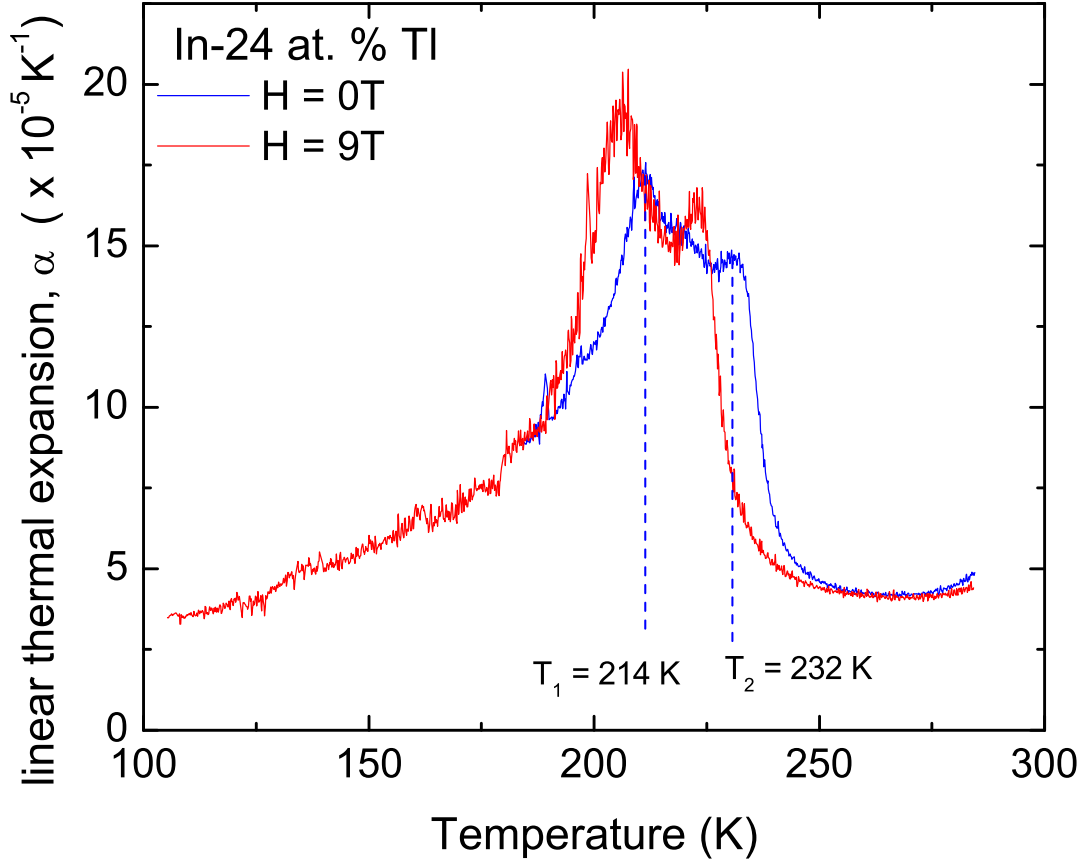


FIG. 1: Magnetic field dependence of the coefficient of linear thermal expansion for In-24 at.% Tl in the vicinity of the MT. The magnetic field is applied at room temperature parallel to the [010] crystallographic axis of the fcc phase. In both cases the data were recorded on cooling from 300 K at a rate of 0.2 K/min.

9 T oriented parallel to the [010] direction of the fcc structure. Two peaks are evident in both the  $H = 0$  T and 9 T data, and the peak structure spans 180 K to 260 K in the  $H = 0$  T data. If one assigns characteristic temperatures to each of these two peaks ( $T_1 = 214$  K and  $T_2 = 232$  K), one sees a that the temperature is reduced ( $T_1 = 205$  K and  $T_2 = 224$  K) in 9 T. Both measurements were repeated on the same crystal, and the peak temperatures did not shift; hence there is no evidence of cycling. With  $H = 9$  T,  $T_1$  is reduced by approximately 6 K and  $T_2$  is reduced by 8 K. The magnitude of the decrease

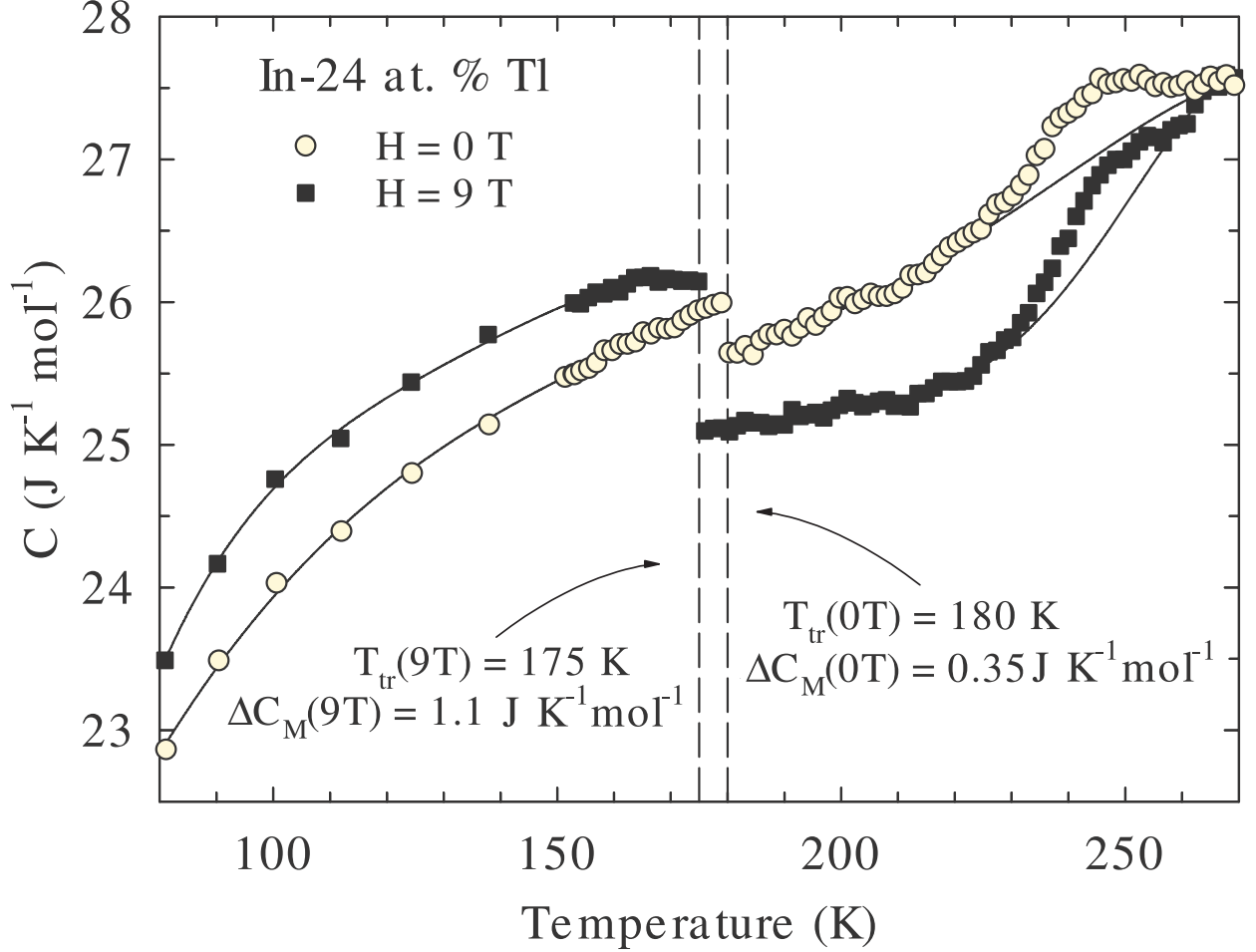


FIG. 2: Magnetic field dependence of the specific heat of In-24 at.% Tl in the vicinity of MT. The magnetic field is applied parallel to the [100] crystallographic axis of the fcc phase. Values for the transition temperatures,  $T_{tr}$ , and the discontinuities in the specific heat evaluated at the MT,  $\Delta C_M$  are shown in the plot. In the absence of the magnetic field the transition occurs at  $T_{tr}(0T)=180$  K, whereas for  $H=9$  T the transition temperature becomes  $T_{tr}(9T)=175$  K.

in the characteristic temperatures roughly correspond to the magnetic-energy scale of an electron in the applied field ( $k_B \Delta T_1 \approx \mu_B H$ ), which implies that the transition intimately involves the conduction electrons. Previous zero-field results of Liu *et al.*<sup>37</sup> show that the slight compression along the [100] direction causes the crystal to transform so that [100] axis remains an  $a$ -axis of the tetragonal structure. The expansivity data shows a less pronounced field dependence when the field is applied in the fcc [001] direction, which is consistent with tetragonal anisotropy. We tentatively identify the [001] direction with the  $c$ -axis by assuming that the lowering of the structural energy is primarily due to electrons near the Bragg planes

closer to the Fermi surface<sup>38</sup> since the Lorentz force from fields perpendicular to the planes should be more effective in changing the electronic structure. Larger changes in electronic binding energy are expected to result in larger changes in the transition temperature.

The reason for the two-peak structure in In-24 at.% Tl is a result of the twinning structure that accompanies the martensitic transition. Video evidence of the development of the transition morphology through the transformation temperature regime for an In-19 at.%Tl alloy shows that over an approximate 25 K temperature range in the vicinity of the martensitic transition, the surface bands appear discontinuously and also thicken as the temperature is decreased<sup>39</sup>. In addition, at a temperature below the MT one set of variants will disappear at the expense of another set, giving rise to the double peak structure. InTl is a soft alloy ( $\Theta_D = 94$  K), and the spring-loaded capacitor imparts a small amount of compressive stress on the sample. This stress then controls the allowed variant morphology accompanying the transition. It should be noted that the anomaly in the measured linear thermal expansion coefficient with temperature is consistent with the measurement direction being predominantly an  $a$ -axis following the cubic-to-tetragonal transition. Comparable behavior has been observed for the anomaly in  $\alpha(T)$  measured by capacitance dilatometry by Liu and coworkers<sup>37</sup>, who also showed that by applying a biaxial stress field to a [100] crystal, perpendicular to the measurement direction, the observed result for the anomaly in  $\alpha(T)$  became  $c$ -axis-like.

### III. SPECIFIC-HEAT MEASUREMENTS

Specific-heat measurements were made on single crystal samples of In-24 at.% Tl, taken from the same batch that was used for the linear-expansion measurements, and polycrystalline samples of the U-26 at.% Nb alloy. Figure 2 shows the results for the specific heat in the vicinity of the MT, measured using a thermal-relaxation method in magnetic fields applied along the [100] direction with field strengths between 0 and 9 T. The specimen was thermally attached to a specimen platform with a thin layer of Apiezon N grease. The specific heat of the empty sample platform and the specific heat of Apiezon N were measured separately and subtracted from the total specific heat to obtain the specific heat of the sample. The performance of the calorimeter was rigorously tested with a variety of conditions and materials confirming its accuracy<sup>40</sup>. In zero magnetic field, anomalous tem-

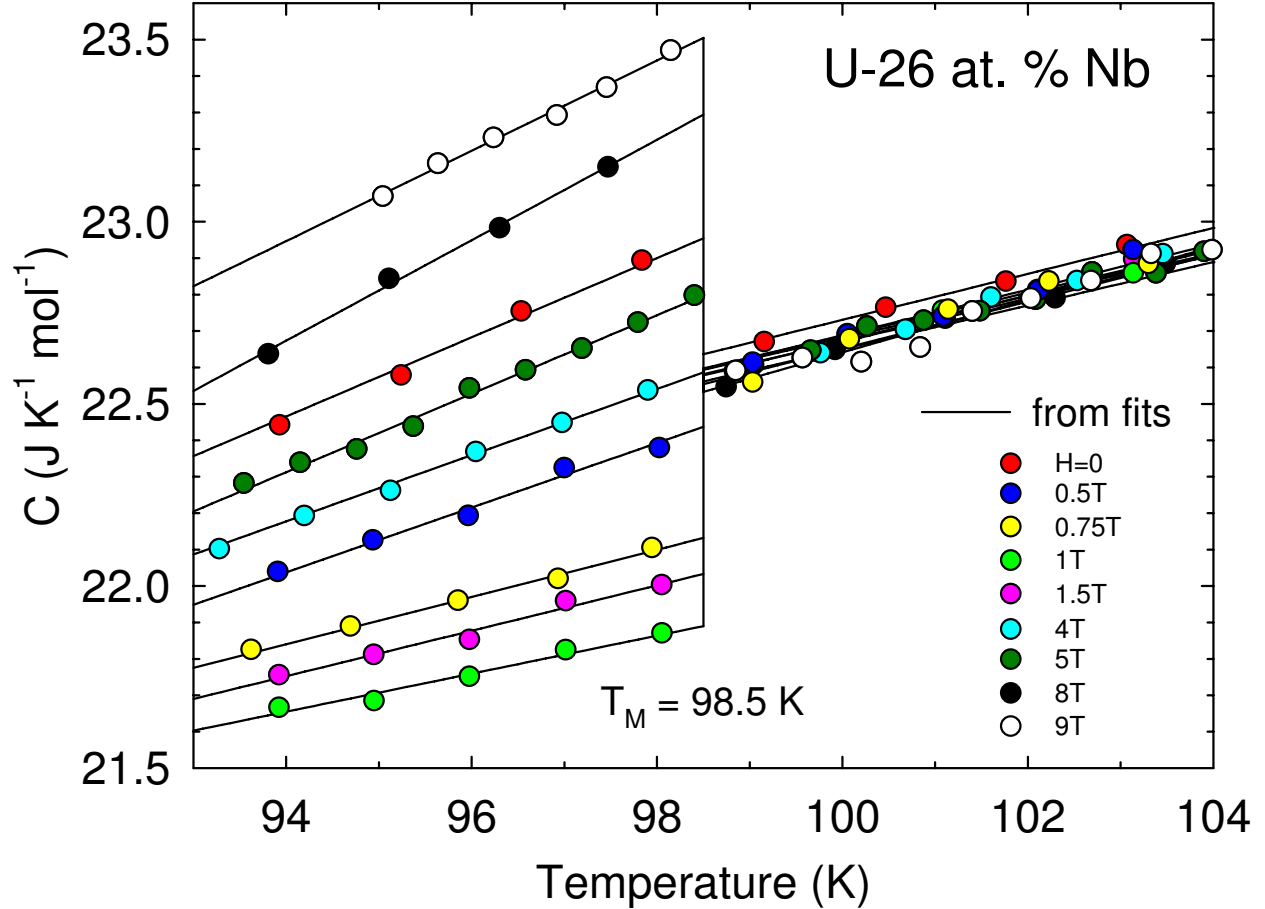


FIG. 3: Specific heat data in the vicinity of the MT in U-26 at.% Nb as a function of magnetic field. All data were recorded on warming.

perature dependence for the specific heat in decreasing temperature is first detected at about 260 K. Then at 180 K there is a clear discontinuity with the specific heat increasing by  $0.31 \text{ J K}^{-1}\text{mol}^{-1}$ . The difference in the martensitic transition temperature between the specific heat and the thermal expansion could be caused by slight changes in the Ti concentration. Application of the magnetic field depresses the temperature of this discontinuity by 5 K, and  $\Delta C_M$  increases by a factor of three to  $1.1 \text{ J K}^{-1}\text{mol}^{-1}$  for  $H = 9 \text{ T}$ . The change of the temperature of the discontinuity with  $H = 9 \text{ T}$  coincides with the observed changes in the characteristic temperatures found in the thermal expansion coefficient. When the 9 T field was applied along another crystallographic axis of the fcc phase, say [001], the measured discontinuity of the specific heat was reduced which, for reasons previously discussed, is consistent with the [001] axis becoming the  $c$ -axis of the tetragonal phase.

Figure 3 shows the specific-heat data in the vicinity of the MT in a U-26 at.% Nb alloy

as a function of magnetic field. Above the transition temperature, all data are congruent to within  $\pm 1\%$ . Linear extrapolations were made over temperatures spanning the MT and were used to derive  $\Delta C_M(H)$ , which has an estimated precision of  $\sim 1\%$ . The negative suppression in the data for fields in the range  $0.3 T \leq H \leq 4 T$  suggests that the magnetic field is relaxing the lattice strain. Because the UNb alloys are polycrystalline and have a low-symmetry orthorhombic structure, microstrain originating from misorientations of grain boundaries are known to affect the low-temperature specific heat and high-temperature specific heat of  $\alpha$ -uranium (also orthorhombic)<sup>41,42</sup>. Above 1 T the field dependence is indicative of a significant change in the heat capacity. We have measured such an effect in the shape-memory alloy AuZn where the opening of a gap at the Fermi surface<sup>25,26</sup> affects the shape of the excess specific heat at the transition temperature.

#### IV. ACOUSTIC MEASUREMENTS

A pulse-echo technique was used to explore the properties of longitudinal sound waves with wave vectors along the [110] direction of the stoichiometric (1:1) AuZn crystal<sup>43,44</sup>. These measurements were made in the temperature range  $0.07 K \leq T \leq 50 K$  with magnetic fields that were varied up to 45 T. The samples were mounted on a single-axis goniometer that allowed the orientation of the sample in the magnetic field to be controlled to within one degree. The relative change in the speed of sound was measured with a precision of  $10^{-7}$ .

In close agreement with the results of Schiltz *et al.*<sup>45</sup>, the speed of longitudinal sound in the [110] direction shows a linear increase with decreasing temperature between room temperature and the transition temperature 64 K. The speed of sound exhibits quantum oscillations, shown in Fig. 4. The magneto-acoustic oscillations in AuZn can be compared with measurements<sup>25,26</sup> of the de Haas-van Alphen oscillations. Previously, it was found that the de Haas-van Alphen effect persisted up to 100 K in pulsed magnetic fields. Since the present study is limited to fields below  $H = 45$  T, the oscillations are only observable up to a maximum temperature of  $\sim 50 K$ . The amplitude of the magneto-acoustic oscillations reaches the largest values when the magnetic field is oriented along the [110] axis. The Fourier spectrum shown in Fig. 5 exhibits peaks at discrete frequencies. This spectrum shows peaks  $\beta$  at 303 T,  $\gamma$  at 1141 T, and  $\delta$  at 4770 T, in accordance with the measurements

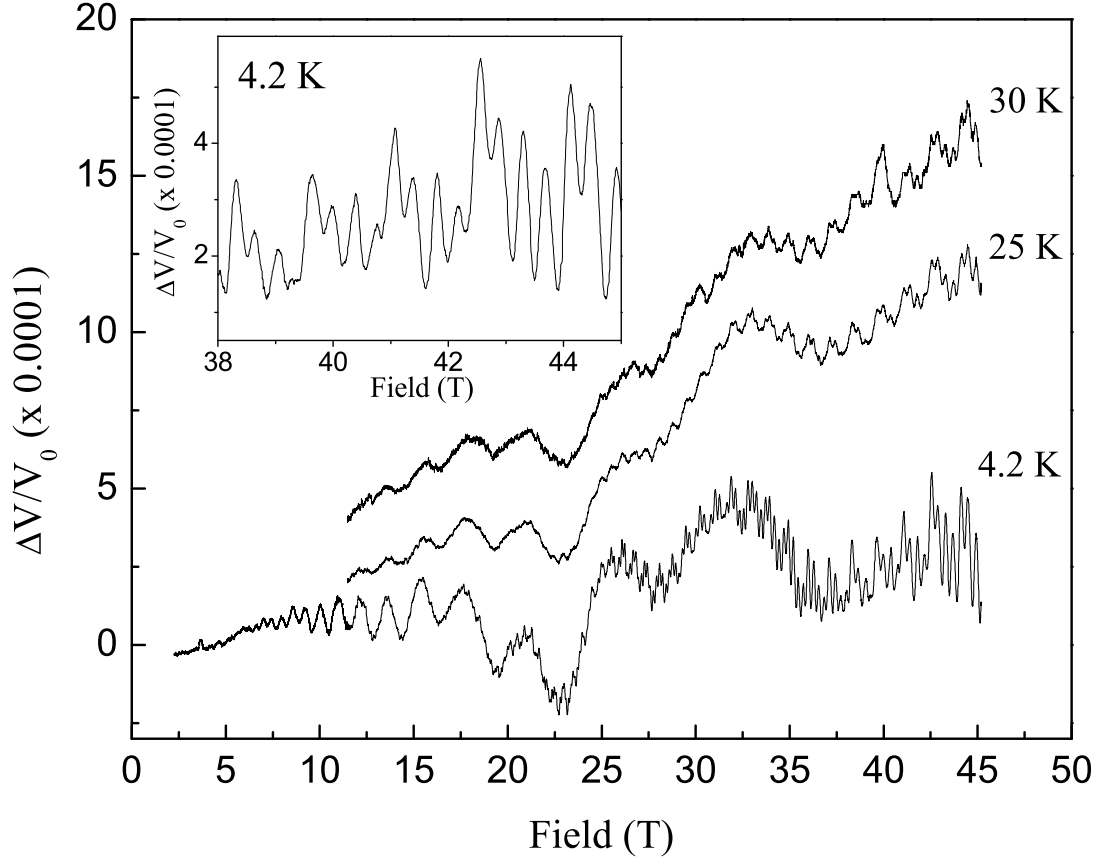


FIG. 4: Oscillations of the speed of sound in AuZn measured at several temperatures in the martensite phase. The inset shows the high-field part of these oscillations. The 60.3 MHz longitudinal sound wave and the field are both directed along  $[110]$  crystallographic direction.

of the de Haas-van Alphen effect<sup>25</sup>. In addition, we also observe the  $\alpha$  peak at 120 T, which was not observed in the de Haas-van Alphen measurements. The oscillations are interpreted in terms of Landau tubes sweeping through the Fermi surface, which produce oscillations in the dielectric constant. The dielectric constant is involved in screening the indirect interactions between the ions and is responsible for their asymptotic Friedel oscillations with wave vector  $2k_F$ <sup>46,47</sup>. The oscillatory dependence of the pair-potential on the magnetic field then produces oscillations of the phonon frequencies. The temperature-dependence of the

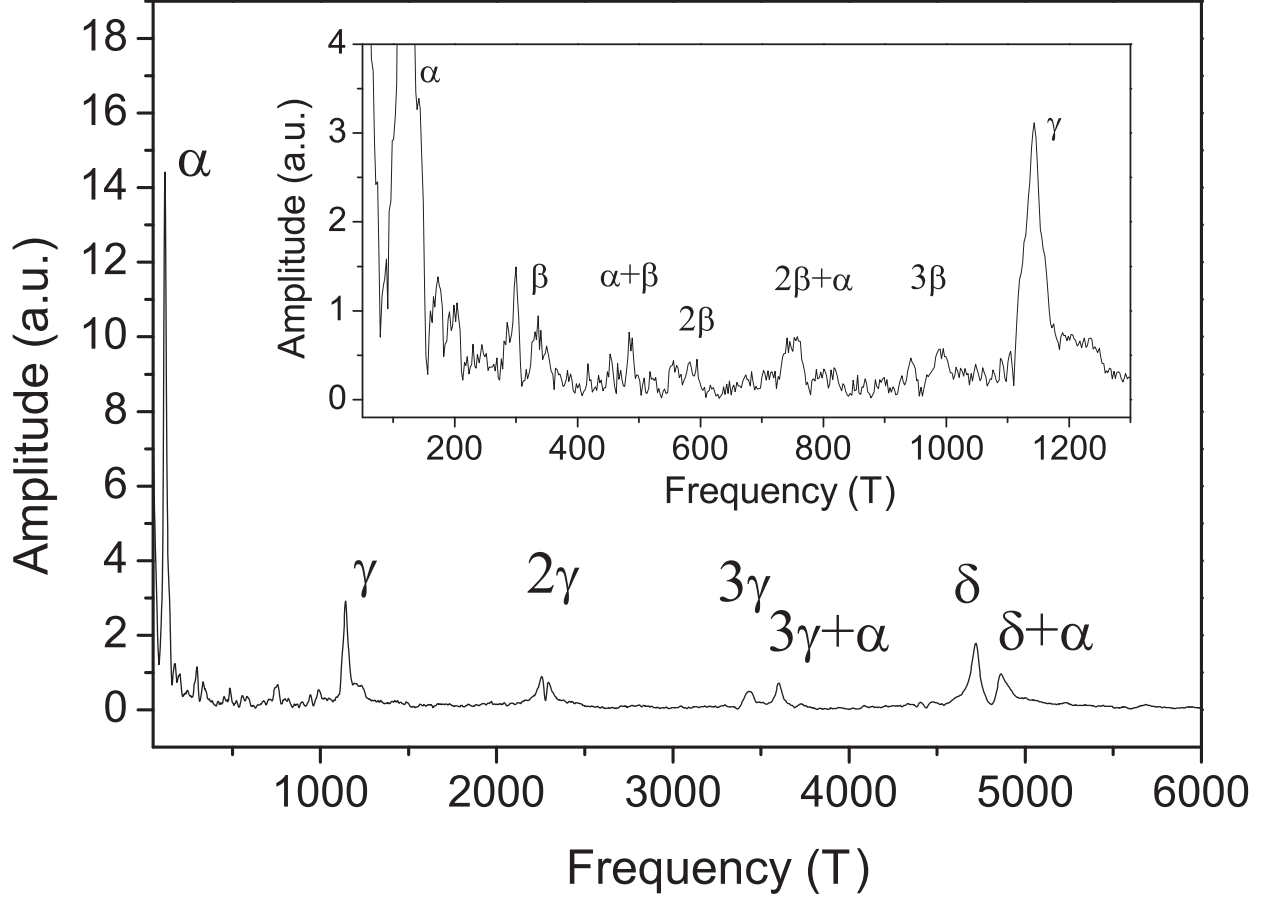


FIG. 5: Fourier image of the 4.2 K oscillations (Fig.4). The inset shows a magnified view of the low-frequency part of the spectrum. Some peaks are split by 46 T, although this frequency was not explicitly detected.

amplitudes of the magneto-acoustic oscillations were fit to the Lifshitz-Kosevitch formula

$$A = \frac{\frac{2\pi^2 m^* c k_B T}{e \hbar B}}{\sinh\left(\frac{2\pi^2 m^* c k_B T}{e \hbar B}\right)} \exp\left[-\frac{2\pi^2 m^* c k_B T_D}{e \hbar B}\right], \quad (2)$$

where  $m^*$  is the effective mass, and  $T_D$  is the Dingle temperature. The effective masses of  $m_\gamma \approx 0.21 \pm 0.01 (m_e)$  and  $m_\delta \approx 0.32 \pm 0.01 (m_e)$  for the  $\gamma$  and  $\delta$  orbits respectively are in agreement with earlier experimental and theoretical predictions for the hexagonal martensite phase<sup>25</sup>. The effective mass for the  $\alpha$  sheet is determined to be  $m_\alpha \approx 0.12 \pm 0.01 (m_e)$ . The Dingle temperatures are estimated as  $T_\alpha \approx 19 \pm 1$  K, while  $T_\gamma \approx 16 \pm 3$  K, and  $T_\delta \approx 16 \pm 1$  K corresponding to cyclotron mean-free paths of the order of 600 Å. This mean-free path is comparable to that inferred from the measured value of the residual resistivity which is  $6.03 \mu\Omega\text{cm}$ . The observation of the  $\alpha$  orbit combined with previous de

Haas-van Alphen measurements on the low temperature phase<sup>25</sup> points to the validity of electronic structure calculations for AuZn. From the measured and calculated orbit of the high-temperature cubic phase, Goddard *et al.* concluded<sup>26</sup> that the Fermi surface is nested with a wave vector oriented along the (111) direction of the cubic Brillouin zone that is nearly commensurate ( $\sim \frac{2}{3}$ ) with Brillouin zone and that the system lowers its energy by undergoing a periodic modulation of the lattice which, via electron-phonon coupling, opens a gap at the Fermi surface. The acoustic de Haas-van Alphen effect supports this conclusion since it not only reproduces some of the measured de Haas-van Alphen frequencies but it is also direct experimental evidence of strong electron-phonon interactions.

## V. CONCLUSIONS

To summarize, we have shown that several materials show evidence that the Fermi-surface electronic structure plays a significant role in MTs. The MT in the bulk thermodynamical properties in nonmagnetic alloys is significantly altered by the application of a magnetic field. In the absence of ordered magnetism these results provide strong evidence that the conduction electrons play an important role in the MT mechanism. This conclusion is further confirmed by the presence of quantum oscillations which represent a direct probe of the Fermi surface. The cross-sectional frequencies observed here are in favorable agreement with previously reported observations<sup>25,26</sup>.

### Acknowledgments

The authors would like to acknowledge Yongbin Lee, Bruce Harmon, and Dan Thoma for useful discussions. The work at Temple was supported by the United States Department of Energy, Office of Basic Energy Sciences, through award DEFG02-01ER45872. The high magnetic field measurements were carried out in Florida at the NHMFL under the auspices of the United States Department of Energy, NSF, and the State of Florida. Ultrasonic research at the NHMFL is supported by the in-house research program. Work at Los Alamos was

performed under the auspices of the United States Department of Energy.

---

- <sup>1</sup> J. Friedel, *J. Phys. Lett. (Paris)* **35**, 59 (1974).
- <sup>2</sup> G. Guénin, M. Morin, P.F. Gobin, W. de Jonghe, and L. Delaey, *Scr. Metall.* **11**, 1071 (1977).
- <sup>3</sup> A. Planes and L. Mañosa, *Solid State Phys.* **55**, 159 (2001).
- <sup>4</sup> M. Mori, Y. Yamada, and G. Shirane, *Solid State Commun.* **17**, 127 (1975).
- <sup>5</sup> A. Nagasawa and Y. Morii, *Mater. Trans. JIM* **34**, 855 (1993).
- <sup>6</sup> W. Petry, A. Heiming, J. Trampenau, M. Alba, C. Herzig, H.R. Schober, and G. Vogl, *Phys. Rev. B* **43**, 10933 (1991); A. Heiming, W. Petry, J. Trampenau, M. Alba, C. Herzig, H.R. Schober, and G. Vogl, *Phys. Rev. B* **43**, 10948 (1991); J. Trampenau, A. Heiming, W. Petry, M. Alba, C. Herzig, W. Miekeley, and H.R. Schrober, *Phys. Rev. B* **43**, 10963 (1991).
- <sup>7</sup> L. Mañosa, J. Zarestky, T. Lograsso, D.W. Delaney, and C. Stassis, *Phys. Rev. B* **48**, 15708 (1993).
- <sup>8</sup> S.M. Shapiro, B.X. Yang, G. Shirane, Y. Noda, and L.E. Tanner, *Phys. Rev. Lett.* **62**, 1298 (1989).
- <sup>9</sup> A. Planes, L. Mañosa, and E. Vives, *Phys. Rev. B* **53**, 3039 (1996).
- <sup>10</sup> K.M. Ho, C.L. Fu, and B.N. Harmon, *Phys. Rev. B* **28**, 6687 (1983); K.M. Ho, C.L. Fu, and B.N. Harmon, *Phys. Rev. B* **29**, 1575 (1984).
- <sup>11</sup> C. Stassis, J. Zarestky, D. Arch, O.D. McMasters, and B.N. Harmon, *Phys. Rev. B* **18**, 2632 (1978).
- <sup>12</sup> G. Guenin, R. Pynn, D. Rios-Jara, L. Delaey, and P.F. Gobin, *phys. stat. sol. (a)* **59**, 553 (1980).
- <sup>13</sup> L. Mañosa, A. Planes, J. Ortín, and B. Martínez, *Phys. Rev. B* **48**, 3611 (1993).
- <sup>14</sup> R.J. Gooding and J.A. Krumhansl, *Phys. Rev. B* **38**, 1695 (1988); R.J. Gooding and J.A. Krumhansl, *Phys. Rev. B* **39**, 1535 (1989); J.A. Krumhansl and R.J. Gooding, *Phys. Rev. B* **39**, 3047 (1989); J.R. Morris and R.J. Gooding, *Phys. Rev. Lett.* **65**, 1769 (1990).
- <sup>15</sup> P.J. Brown, J. Crangle, T. Kanomata, M. Matsumoto, K.-U. Neumann, B. Ouladdiaf, and K.R.A. Ziebeck, *J. Phys. C.M.* **14**, 10159 (2002).
- <sup>16</sup> D.G. Pettifor, *J. Phys. C* **3**, 367 (1970).
- <sup>17</sup> J. Ihm and M.L. Cohen, *Phys. Rev. B* **23**, 1576 (1981).
- <sup>18</sup> A.K. McMahan and J.A. Moriarty, *Phys. Rev. B* **27**, 3235 (1983).

- <sup>19</sup> L.A. Grifalco, *Acta Metall.* **24**, 247 (1970).
- <sup>20</sup> J. Hafner, *From Hamiltonians to Phase Diagrams*, Springer Series in Solid State Sciences 70, Springer Verlag, Berlin 1987.
- <sup>21</sup> W. Hume-Rothery, *Adv. in Physics* **3**, 149 (1954).
- <sup>22</sup> H. Jones, *Proc. Phys. Soc. A* **49**, 250 (1937).
- <sup>23</sup> V. Heine and D. Weaire, *Solid State Physics*, Volume 22 Academic Press, N.Y. (1970).
- <sup>24</sup> W.G. Burgers, *Physica Utrecht* **1**, 561 (1934).
- <sup>25</sup> R.D. McDonald, J. Singleton, P.A. Goddard, F. Drymiotis, N. Harrison, H. Harima, M.T. Suzuki, A. Saxena, T. Darling, A. Migliori, J.L. Smith, and J.C. Lashley, *J. Phys. Cond. Mat.* **17**, L69, (2005).
- <sup>26</sup> P.A. Goddard, J. Singleton, R.D. McDonald, N. Harrison, J.C. Lashley, H. Harima, and M.-T. Suzuki, *Phys. Rev. Lett.* **94**, 116401 (2005).
- <sup>27</sup> G.L. Zhao and B.N. Harmon, *Phys. Rev. B* **45**, 2818, (1992); G.L. Zhao and B.N. Harmon, *Phys. Rev. B* **48**, 2031, (1993).
- <sup>28</sup> S.K. Satija, S.M. Shapiro, M.B. Salamon, and C.M. Wayman, *Phys. Rev. B* **29**, 6031 (1984); S.M. Shapiro, J.Z. Larese, Y. Noda, S.C. Moss, and L.E. Tanner, *Phys. Rev. Lett.* **57**, 3199, (1986).; T. Ohba, S.M. Shapiro, S. Aoki, and K. Otsuka, *Jpn. J. Appl. Phys.* **33**, L 1631 (1994).
- <sup>29</sup> A. Landa, J. Klepeis, P. Soderlind, I. Naumov, O. Velikokhatnyi, L. Vitos, and A. Ruban, *J. Phys. Cond. Mat.* **18**, 5079 (2006).
- <sup>30</sup> S.B. Dugdale, R.J. Watts, J. Laverock, Zs. Major, M.A. Alam, M. Samsel-Czekala, G. Kontrym-Sznajd, Y. Sakurai, M. Itou, and D. Fort, *Phys. Rev. Lett.* **96**, 046406 (2006).
- <sup>31</sup> D. Shoenberg, *Magnetic Oscillations in Metals*, Cambridge University Press (1984).
- <sup>32</sup> T.R. Finlayson and H.G. Smith, *Metall. Trans. A* **19**, 193 (1988).
- <sup>33</sup> G. M. Schmiedeshoff, A. W. Lounsbury, D. J. Luna, S. J. Tracy, A. J. Schramm, S. W. Tozer, V. F. Correa, S. T. Hannas, T. P. Murphy, E. C. Palm, A. H. Lacerda, J. L. Smith, J. C. Lashley, and J. C. Cooley, *Rev. Sci. Instrum.*, **77** 123907 (2006).
- <sup>34</sup> R.W. Meyerhoff and J. F. Smith, *Acta. Met.* **11**, 529 (1963).
- <sup>35</sup> V. Heine and D. Weaire, *Phys. Rev.* **152**, 603 (1966).
- <sup>36</sup> J. W. Stout and L. Guttman, *Phys. Rev.*, **88**, 713 (1952).
- <sup>37</sup> M. Liu, T.R. Finlayson, and T.F. Smith, *Phys. Rev. B* **48**, 3009 (1993).
- <sup>38</sup> G.B. Brandt and J.A. Rayne, *Phys. Rev.* **132**, 1512 (1982), see also N.W. Ashcroft and W.E.

- Lawrence, Phys. Rev. **174**, 938 (1968).
- <sup>39</sup> The video is available for viewing on the internet at [www.physics.monash.edu/research/instsoli/InTI](http://www.physics.monash.edu/research/instsoli/InTI)
- <sup>40</sup> J.C. Lashley, M.F. Hundley, A. Migliori, J.L. Sarrao, P.G. Pagliuso, T.W. Darling, M. Jaime, J.C. Cooley, W.L. Hults, L. Morales, D.J. Thoma, J.L. Smith, J. Boerio-Goates, B.F. Woodfield, G.R. Stewart, R.A. Fisher, and N.E. Phillips, Cryogenics **43**, 369 (2003).
- <sup>41</sup> B. Mihaila, C.P. Opeil, F.R. Drymiotis, J.L. Smith, J.C. Cooley, M.E. Manley, A. Migliori, C. Mielke, T. Lookman, A. Saxena, A.R. Bishop, K.B. Blagoev, D.J. Thoma, J.C. Lashley, B.E. Lang, J. Boerio-Goates, B.F. Woodfield, and G.M. Schmiedeshoff, Phys. Rev. Lett. **96**, 076401 (2006).
- <sup>42</sup> M.E. Manley, M. Yethiraj, H. Sinn, H.M. Volz, A. Alatas, J.C. Lashley, W.L. Hults, G.H. Lander, and J.L. Smith, Phys. Rev. Lett. **96**, 125501 (2006).
- <sup>43</sup> T.W. Darling, F. Chu, A. Migliori, D.J. Thoma, M. Lopez, J.C. Lashley, B.E. Lang, J. Boerio-Goates, and B.F. Woodfield, Phil. Mag. B **82**, 825 (2002).
- <sup>44</sup> O. Svitelskiy, A. Suslov, J. Singleton, and J. C. Lashley, CP850, AIP Conference Proceedings *Low Temperature physics: 24<sup>th</sup> International Conference on Low Temperature Physics LT-24*, (Y. Takano, S. P. Hershfeld, S. O. Hill, P. J. Hershfeld, and A. M. Goldman eds.), p. 1319 (2006).
- <sup>45</sup> R. Schiltz, T. Prevender, and J. Smith, J. Appl. Phys. **42**, 4680 (1971).
- <sup>46</sup> M.H. Cohen in *Metallic Solid Solutions*, (J. A. Friedel and A. Guinier eds.) Benjamin, New York (1962).
- <sup>47</sup> W.A. Harrison *Pseudopotentials in the Theory of Metals*, Benjamin, New York (1966).